Logarithmic behavior of the conductivity of electron-beam deposited granular Pt/C nanowires

L. Rotkina,[1,3,*] S. Oh,[2,†] J. N. Eckstein,[2] and S. V. Rotkin[3]
[1]*Beckman Institute, UIUC, 405 N. Mathews, Urbana, Illinois 61801, USA*
[2]*Department of Physics, UIUC, 1110 W. Green, Urbana, Illinois 61801, USA*
[3]*Department of Physics, Lehigh University, 16 Memorial Dr. E., Bethlehem, Pennsylvania 18015, USA*
(Received 25 October 2005; published 21 December 2005)

We found that granular Pt/C composite nanowires have a logarithmic temperature dependence of conductivity in a wide range of temperatures. The logarithmic dependence can be explained by Coulomb interaction between Pt grains in a conductive carbon matrix. We stress the difference of the conductivity mechanism in the composite nanogranular material and known mechanisms in bulk metals/semiconductors and low-dimensional systems, including logarithmic dependence in systems with two-dimensional weak localization. Our observations show that local voltage fluctuations between grains result in the $\log(T)$ dependence for the samples with high conductivity (annealed nanowires), while the samples with low conductivity (as fabricated nanowires) appear to be insulators with a Coulomb gap.

DOI: 10.1103/PhysRevB.72.233407 PACS number(s): 73.23.Hk, 81.07.Bc, 81.40.Rs

We have realized a granular composite material, which exhibits clearly Coulomb intergrain correlations. This is supported by an observation of a logarithmic temperature dependence of the conductivity of a three-dimensional (3D) sample in a wide range of temperature.

The $\log(T)$ dependence is commonly observed in two-dimensional (2D) disordered metal films[1] and explained theoretically decades ago.[2] Weak localization corrections to a 2D Drude conductivity diverge as $\log(T)$ at low temperatures.[3] However, we dealt with a 3D system, because the size of a single Pt grain in our material is much smaller than the wire width and thickness (see below). Thus the transport happens via the whole volume of the nanowire. In addition, we measured the $\log(T)$ dependence up to 200 K. All these observations rule out the applicability of the 2D weak localization model to explain our experimental data. We found our experimental data to be consistent with a theoretical model of conductivity in a granular metal.[4,5] The $\log(T)$ dependence has been found earlier in granular superconductor cermet films,[6] soft magnetic heterogenous alloys,[7] and Al-Ge films.[8]

Granular materials are interesting because they provide a possibility of reaching the limit of pure Coulomb correlations. There is a temperature range where the quantum interference is broken by a thermal dephasing but the local intergrain voltage fluctuations are present. Even though the dimensionless conductance (between grains) is not very low: $g_o \sim 0.5-0.6$ (in units $2e^2/h$), the spacing between energy levels in a single grain, δ, is small enough (of the order of a few meV) to prove the transport to be incoherent for the temperature: $kT > g_o\delta$. Most important, recent theoretical study showed that the quantum interference correction to the conductivity of a 3D granular metal may be small as compared to the Coulomb intergrain correlations for the whole range of temperatures.[5] Then the voltage fluctuations between neighbor grains determine the transport.

We speculate on our observation of the effect of Coulomb interactions on the conductivity in the nanogranular composite material. We emphasize the (1) low (semimetallic) resistivity of the matrix; (2) a high crystallinity and, thus, high conductivity of a single Pt grain; and (3) a small grain size: $D \sim 2-3$ nm. A Coulomb energy of the single grain is of the order of

$$\frac{e^2}{D} \sim 0.5\text{eV} \gg kT.$$

One may expect to observe a Coulomb blockade in a single grain experiment, which is not the case for the nanowire because of the low resistivity of the carbon matrix. The specific resistivity of amorphous carbons can vary by at least three orders of magnitude, ranging from semimetals to semiconductors and depending on the size of the particles (flakes, in case of graphite), the extent of the porosity, the heat treatment, and other factors (see Ref. 9, e.g., and references therein). Because the resistivity of the carbon matrix is not too high in our samples, the strong coupling between the grains washes out the Coulomb blockade effect, and theory predicts an exponential renormalization of the characteristic temperature corresponding to the Coulomb gap.[10] Indeed, we observed a good metallic conduction for the whole range of temperatures for the samples with the low resistivity of the matrix.

We have used an electron beam induced deposition (EBID) for fabricating the Pt/C composite nanowires; the method has been detailed in our earlier paper.[11] The process is based on a decomposition of an organometallic precursor by the electron beam close to the surface and sculpturing the wires along the trace of the beam.[12–14] Compared to an electron-beam lithography, the process does not require any electron sensitive layer to be deposited. The patterning occurs at the vacuum-surface interface by a localized chemical vapor deposition (CVD) induced by incident and secondary electrons.[14–16] This approach allows for the formation of various structures, in just a single processing step, with the resolution comparable to the one of the patterns defined by the electron-beam lithography.[17] The decomposition reaction happens under the constantly maintained vacuum and all

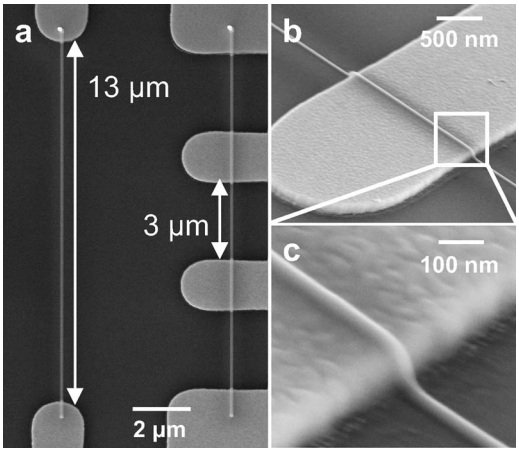

FIG. 1. A SEM micrograph of the Pt/C composite nanowires deposited over the Si/Si_3N_4 substrate with the premanufactured Au/Ti leads: (a) the circuit layout for two-probe and four-probe transport measurements. (b) and (c) The magnified SEM images taken at 52° to the sample surface. Bar sizes are 2 μm (a), 500 nm (b), and 100 nm (c).

volatile by-products as well as small particles produced above the substrate surface are pumped out of the chamber.

We fabricated our circuits directly over the Si/Si_3N_4 substrate with premanufactured Au/Ti leads in the layout shown on the micrographs taken by scanning electron microscopy (SEM) [Fig. 1(a)]. Figures 1(b) and 1(c) present the SEM images of the wires as they connect to the leads, which were taken at 52° to the sample surface to show the 3D geometry of the nanowires. To extract a contact resistance between the gold electrodes and the wires we performed both two-probe and four-probe measurements, and the contact resistance was always immeasurably small as compared to the nanowire resistance.

The transport study was combined with a material study. We have prepared two additional sets of samples: one set on the Cu grid with whiskers of the Pt/C composite material and another one on the Si_3N_4 membrane with Au electrodes and the nanowire crossing the gap between electrodes. Those samples were heat treated *in situ* in a transmission electron microscope (TEM) and the cross-sectional high resolution TEM (HRTEM) imaging followed each step. A high resistance of as-deposited material can be explained by combining the transport measurements (see below) and the results on the structural study presented next.

Diffraction of electrons, obtained simultaneously with the cross-sectional HRTEM, shows the polycrystalline structure of Pt. Pt aggregates in the clusters with an average diameter about 2 nm, and the carbon forms the matrix which is structureless and nonuniform. To stabilize the structure of the wires and remove possible precipitated untreated organic precursor and hydrocarbon debris we performed a series of heat treatments. The cross-sectional HRTEM images taken before and after the annealing show the structure modification (Fig. 2, left, before; right, after). Heat treated material shows more contrast in polycrystalline diffraction patterns. The proportional content of Pt and C has also changed: more Pt and less C are observed, which continues until all volatile

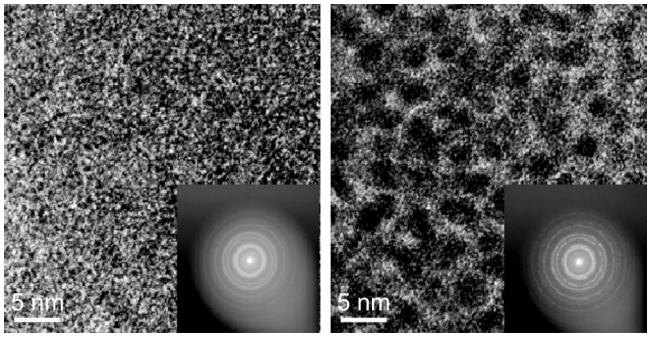

FIG. 2. HRTEM micrographs of the Pt/C nanowire, deposited onto a Si_3N_4 membrane: (left) the image of as deposited material; (right) the image taken after the thermal annealing. Darker regions indicate the Pt crystallites, the bar sizes are 5 nm. The insets show the diffraction patterns.

species and hydrocarbon debris are gone. Though we always registered more intensive Pt peak in the energy dissipative x-ray (EDX) spectra from the heat treated material, it is difficult to speculate on the exact quantities of the elements compared to the x-ray microanalysis spectra of treated and untreated samples. We visually observed a moderate increase of the size of Pt clusters on the HRTEM images. Also a size histogram based on the crystallography (as detailed elsewhere[18]) shows the diameter increase up to 5% for the highest temperature we have applied for the heat treatment (600 °C for TEM samples).

We applied a similar thermal treatment, a rapid thermal annealing (RTA), to the identical sample set prepared for the transport study. The RTA is a conventional technique to stabilize properties of layered structures and decrease a contact resistance for semiconductor circuits (see, e.g., Ref. 19). We exploited the RTA in the inert atmosphere for two reasons: *to improve the contacts* and *to stabilize the composition for the wire's material*.

A drastic resistance drop has been observed as shown in Fig. 3. The resistance, however, was found to be the same in two-probe and four-probe measurements and, thus, this effect is independent of the contact resistance. For our experiment we have prepared 16 identical wires (eight in four-probe and eight in two-probe geometry) and run a series of annealing sessions, 60 seconds each, starting at 200 °C (473 K) up to 500 °C (773 K) with a 100° step. After each annealing step we performed the resistivity measurement at room temperature in a micromanipulator stage. The current-voltage characteristic was linear within the bias range ±250 mV. A high input impedance ($>200\ T\,\Omega$) electrometer (Keithley 617) has been used for highly resistive wires and a sensitive voltmeter (Keithley 182) has been used for less resistive ones with an appropriate current biasing (Keithley 220). The results are summarized on Fig. 3: the initial resistivity of the nanowire was high (20–100 Ω cm). The annealing resulted in the reproducible dramatic decrease of the resistivity down to a few mΩ cm (four orders of magnitude drop). The resistivity which we plot in Fig. 3 is evaluated from the measured resistance assuming that the cross section of the wire is 80 nm $\times$ 80 nm and it does not change during the annealing. Although after the annealing the wire is still more resistive

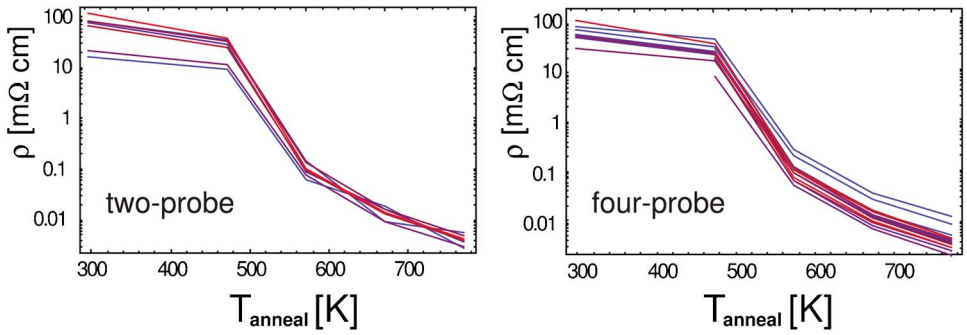

FIG. 3. (Color online) The influence of the rapid thermal annealing on the wire resistivity: (left) two-probe and (right) four-probe room-temperature resistivity vs the annealing temperature. The source-drain voltage was 50 mV, which is within the linear current-voltage characteristics of the nanowires. The resistivity of ~20–100 Ω cm for as-deposited wires decreased by four orders of magnitude with progressive thermal annealing up to 500 °C. Both panel show consistent changes, which proves the effect to be independent of contact resistance.

than typical conductors (4 mΩ cm at room temperature), such drastic resistivity drop is worth more explanation.

After the last annealing (500 °C) had been performed, we wire-bonded one of the nanowires to a ceramic chip carrier and measured the temperature dependence of its resistivity from the room temperature down to 4 K in four-probe geometry (the inset of Fig. 4). We found that even after the annealing the nanowire has not reached true metallic regime: the nanowire resistivity slowly increases as the temperature drops and at 4 K it becomes three times bigger than the room temperature value. We conclude that the material is still far from a bulk pure metal, which is consistent with the granular structure registered by the cross-sectional HRTEM and the polycrystalline diffraction patterns. Even if the resistivity has dropped by four orders of magnitude, it is still 1000 times bigger than the resistivity of the pure platinum (~2 μΩ cm). For an electron density of the pure platinum, $n=6\times10^{22}$ cm^{-3}, the Ioffe-Regel-Mott criterion[20] gives a lower bound for a metallic (Drude) resistivity: $\rho \leqslant 1$ mΩ cm. Therefore, by reducing the resistivity by an order of magnitude our nanowires might show the metallic behavior. This is consistent with our results for the ion beam deposited Pt nanowires that had the room temperature resistivity of 500 μΩ cm or less and showed the metallic dependence of the resistivity vs the temperature,[21] unlike the more resistive electron beam assisted nanowires studied in this work. This high resistivity of the nanowire also means that the electron mean free path is much smaller than the width and the height of the nanowire, which proves *a posteriori* our assumption on the three-dimensional (3D) [vs one-dimensional (1D) transport].

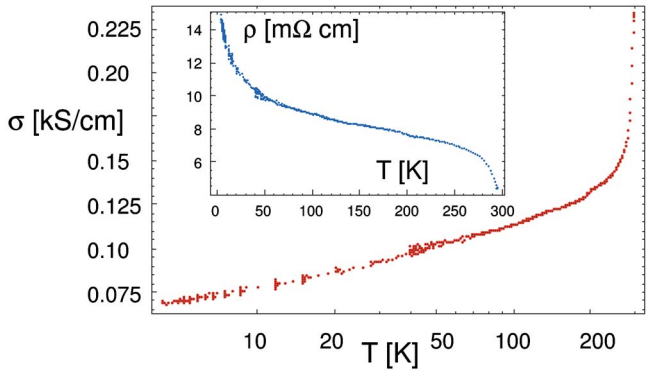

FIG. 4. (Color online) (Main panel) The logarithmic temperature dependence of the conductivity of the annealed nanowire. (Inset) The raw experimental data on resistivity vs T (from the room temperature down to 4 K in four-probe geometry). The source-drain voltage was 50 mV and the log(T) dependence was observed in a wide range of T—up to 200 K.

Figure 4 shows the nanowire conductivity which diverges as log(T) below 200 K. We conclude therefore that the resistivity of our samples is due to neither the intrinsic properties of the Pt crystallites nor the carbon matrix itself. We interpret our transport measurements by the Coulomb blockade effect renormalized in a presence of the conductive matrix. The bare (nonrenormalized) Coulomb energy, $E_c \sim 0.5$ eV, is large because of the small grain size of a few nanometers and it is almost constant during the annealing. In contrast, the renormalized gap E_c^*, which depends exponentially on the matrix conductivity,[10,22,23] may vary significantly. Thus one can measure the strength of Coulomb correlations in the sample by changing the matrix properties.

We conclude that g_o, the bare conductance of the matrix, controls the transport properties of the composite granular material. For high enough g_o, the metallic conduction was measured. One would expect to achieve a metal-insulator transition by decreasing g_o, as it happens in 3D disordered systems[3,6] and also granular metals.[4,5,7,8,24–26] Fortunately, our fabrication technique allows making samples and measuring transport in both high-g and low-g regimes. The insulating behavior was indeed observed for the samples with the lower conductivity. The Coulomb blockade was clearly present in other samples at low temperatures and the trace of it can be seen up to 50 K.[11]

As-fabricated composite material has less crystallinity and, likely, stronger disorder. By thermal post-treatment we improved the structure as documented above. This reflected in an improvement of the transport properties as well: the giant drop of the resistivity followed the annealing. This drastic difference in the transport behavior before and after RTA is due to the conductance of the matrix is close to a critical one, $g_o \simeq g_c$, as defined by the ratio of the Coulomb

energy and the energy level spacing in the grain. According to recent papers[4,5] the critical dimensionless conductance is

$$g_c \sim \frac{1}{6\pi} \log\left(\frac{E_c}{\delta}\right).$$

Using our experimental data on the grain size and material properties we estimate the critical value as $g_c \sim 0.2$. We independently measure in transport experiments in our samples the values of g_o of the same order of magnitude (to be detailed in Ref. 18). Thus, it is likely that the annealing can change the conduction regime. By measuring the temperature dependence of the transport in the granular material before and after the thermal treatment we were able to trace the transition from a granular Coulomb insulator to a granular marginal metal.

Although most of theoretical models assume regular lattice of grains with the same coupling constants, we found that in a real system, with certain, though narrow, distribution of the grain size and intergrain distance, the similar fluctuations develop. This results in the $\log(T)$ dependence of the conductivity that can be clearly seen in our experiment for the temperatures up to 200 K (Fig. 4). Recently, the case of random capacitance and tunneling couplings between the grains has been addressed in the modeling a percolation in the two-dimensional (2D) array,[26] and the conclusion was drawn that the $\log(T)$ dependence still holds for moderately random systems in the metallic regime.

In conclusion, we used an electron beam assisted deposition of Pt to fabricate granular Pt/C composite nanowires. The logarithmic temperature dependence of the conductivity has been observed in the wide range of temperatures for the annealed nanowires. We stressed the difference of the conductivity mechanism in the 3D composite nanogranular material and the weak localization in 2D metals and/or semiconductors. The log dependence of the conductivity for the samples with the high matrix conductance (annealed nanowires) results from the local voltage fluctuations between the grains, while the samples with the low matrix conductance (as fabricated nanowires) have a few orders of magnitude lower conductivity. We found that the size of the Pt grains, their crystal structure, and intergrain distance are almost constant during the annealing. Therefore we attribute the giant drop of the resistivity to the modification of the carbon matrix. The conductance of as grown matrix is close to the critical one. The annealing improves the intergrain conductivity and transforms the Coulomb insulator into the granular metal. We note that additional experiments will be needed to separate the contributions to g_o from the bulk conductivity of the carbon matrix and from the interface between a Pt grain and the matrix.

Experimental part of work was carried out in the Center for Microanalysis of Materials (CMM), UIUC, which is partially supported by the U.S. Department of Energy under Grant No. DEFG02-91-ER45439. We acknowledge the CMM staff members Mike Marshall and Ray Twesten for their supportive assistance with the microscopy. LR and SVR acknowledge the National Science Foundation for partial support under Grant No. ECS 0403489.

*Corresponding author. E-mail: rotkina@uiuc.edu. Present address: Center for Advanced Materials and Nanotechnology, Lehigh University, 5 East Packer Ave., Bethlehem, Pennsylvania 18015, USA.

†Present address: National Institute of Standards and Technology, 325 Broadway, Boulder, Colorado 80305, USA.

[1] G. J. Dolan and D. D. Osheroff, Phys. Rev. Lett. **43**, 721 (1979); R. S. Markiewicz, and L. A. Harris, *ibid.* **46**, 1149 (1981).

[2] P. A. Lee and T. V. Ramakrishnan, Rev. Mod. Phys. **57**, 287 (1985).

[3] E. Abrahams, P. W. Anderson, D. C. Licciardello, and T. V. Ramakrishnan, Phys. Rev. Lett. **42**, 673 (1979).

[4] K. B. Efetov and A. Tschersich, Phys. Rev. B **67**, 174205 (2003).

[5] I. S. Beloborodov, K. B. Efetov, A. V. Lopatin, and V. M. Vinokur, Phys. Rev. Lett. **91**, 246801 (2003).

[6] R. W. Simon, B. J. Dalrymple, D. Van Vechten, W. W. Fuller, and S. A. Wolf, Phys. Rev. B **36**, 1962 (1987).

[7] H. Fujimori, S. Mitani, S. Ohnuma, T. Ikeda, T. Shima, and T. Masumoto, Mater. Sci. Eng., A **181–182**, 897 (1994).

[8] A. Gerber, A. Milner, G. Deutscher, M. Karpovsky, and A. Gladkikh, Phys. Rev. Lett. **78**, 4277 (1997).

[9] K. Kinoshita, *Carbon, Electrochemical and Physicochemical Properties* (John Wiley & Son, Inc., New York, 1988).

[10] K. A. Matveev, Phys. Rev. B **51**, 1743 (1995); Y. V. Nazarov, Phys. Rev. Lett. **82**, 1245 (1999) and references therein.

[11] L. Rotkina, J.-F. Lin, and J. P. Bird, Appl. Phys. Lett. **83**, 4426 (2003).

[12] S. Matsui and K. Mori, J. Vac. Sci. Technol. B **4**, 299 (1986).

[13] H. W. P. Koops, R. Weiel, and D. P. Kern, J. Vac. Sci. Technol. B **6**, 477 (1988).

[14] S. Matsui and T. Ichihashi, Appl. Phys. Lett. **53**, 842 (1988).

[15] H. W. P. Koops, A. Kaya, and M. Weber, J. Vac. Sci. Technol. B **13**, 2400 (1995).

[16] N. Silvis-Cividjian, C. W. Hagen, P. Kruit, M. A. J. v.d. Stam, and H. B. Groen, Appl. Phys. Lett. **82**, 3514 (2003).

[17] K. Mitsuishi, M. Shimojo, M. Han, and K. Furuya, Appl. Phys. Lett. **83**, 2064 (2003).

[18] L. Rotkina (unpublished).

[19] W.-K. Chen, *The VLSI Handbook* (CRC Press, Boca Raton, FL, 1999).

[20] A. F. Ioffe and A. P. Regel, Prog. Semicond. **4**, 237 (1960); N. F. Mott, *Metal-Insulator Transitions* (Taylor & Francis, London, 1990).

[21] J.-F. Lin, J. P. Bird, L. Rotkina, and P. A. Bennett, Appl. Phys. Lett. **82**, 802 (2003).

[22] S. V. Panyukov and A. D. Zaikin, Phys. Rev. Lett. **67**, 3168 (1991).

[23] X. Wang and H. Grabert, Phys. Rev. B **53**, 12621 (1996).

[24] M. Bowman, A. Anaya, A. L. Korotkov, and D. Davidovic, Phys. Rev. B **69**, 205405 (2004).

[25] L. H. Yu and D. Natelson, Phys. Rev. B **68**, 113407 (2003).

[26] M. V. Feigel'man, A. S. Ioselevich, and M. A. Skvortsov, Phys. Rev. Lett. **93**, 136403 (2004).